

Super-allowed α decay above doubly-magic ^{100}Sn and properties of $^{104}\text{Te} = ^{100}\text{Sn} \otimes \alpha$

P. Mohr^a

Diakoniekrankehaus, D-74523 Schwäbisch Hall, Germany

Received: 15 November 2006 / Revised: 20 December 2006

Published online: 25 January 2007 – © Società Italiana di Fisica / Springer-Verlag 2007

Communicated by W. Nazarewicz

Abstract. α -decay half-lives for $^{104,105,106}\text{Te}$ and $^{108,109,110}\text{Xe}$ close above the doubly-magic ^{100}Sn are calculated from systematic double-folding potentials. The derived α preformation factors are compared to results for $^{212,213,214}\text{Po}$ and $^{216,217,218}\text{Rn}$ above the doubly-magic ^{208}Pb . α -decay energies of $Q_\alpha = 5.42 \pm 0.07$ MeV and 4.65 ± 0.15 MeV are predicted for ^{104}Te and ^{108}Xe ; the corresponding half-lives are $T_{1/2} \approx 5$ ns for ^{104}Te and of the order of $60 \mu\text{s}$ for ^{108}Xe . Additionally, the properties of rotational bands in ^{104}Te are analyzed, and the first excited 2^+ state in ^{104}Te is predicted at $E_x = 650 \pm 40$ keV; it decays preferentially by γ emission with a reduced transition strength of 10 Weisskopf units to the ground state of ^{104}Te and with a minor branch by α emission to the ground state of ^{100}Sn .

PACS. 21.10.-k Properties of nuclei; nuclear energy levels – 21.10.Tg Lifetimes – 27.60.+j $90 \leq A \leq 149$ – 21.60.Gx Cluster models

1 Introduction

Studies of α -decay properties of nuclei with $Z \approx N$ in the mass region above $A \approx 100$ have been stimulated by recent experimental progress: Seweryniak *et al.* [1] have detected the α -decay of ^{105}Te at the Argonne fragment analyzer, and Liddick *et al.* [2] have analyzed the α -decay chain $^{109}\text{Xe}(\alpha)^{105}\text{Te}(\alpha)^{101}\text{Sn}$ at the recoil mass spectrometer of the Holifield radioactive ion beam facility. In both papers the measured α -decay half-lives are interpreted as indication for super-allowed α -decay in the vicinity of the doubly-magic nucleus ^{100}Sn with $Z = N = 50$. Whereas the larger experimental uncertainties in [1] allowed only to conclude “a modest enhancement of α -decay rates toward the $N = Z$ line”, the latest data of [2] clearly confirm the super-allowed α -decay of ^{105}Te by comparison with the analogous α -decay of ^{213}Po . A first theoretical report by Xu and Ren [3] is based on improved folding potentials, and they find an increased α preformation factor for $N = Z$ nuclei.

The present study reanalyzes the new experimental data [1,2] using a similar model as [3] in combination with double-folding potentials which are close to the results of elastic scattering data on $N \approx Z$ data in the $A \approx 100$ mass region (^{92}Mo [4], ^{106}Cd [5], ^{112}Sn [6]). The results further confirm the super-allowed α -decay around ^{100}Sn . The systematic properties of the double-folding potentials allow a prediction of the α -decay energy of ^{104}Te

and ^{108}Xe with relatively small uncertainties. However, the prediction of the α -decay half-lives has still considerable uncertainties because of the exponential dependence on the α -decay energy. In addition, α cluster properties of the nucleus $^{104}\text{Te} = ^{100}\text{Sn} \otimes \alpha$ can be predicted in a similar way as in [7,8] for $^{94}\text{Mo} = ^{90}\text{Zr} \otimes \alpha$. In particular, the excitation energy of the first excited 2^+ state in ^{104}Te and its decay properties by γ and α emission are calculated. These decay properties have noticeable influence on the experimental determination of the α -decay of ^{104}Te .

2 α -decay half-lives

In a semi-classical approximation the α -decay width Γ_α is given by the following formulae [9]:

$$\Gamma_\alpha = PF \frac{\hbar^2}{4\mu} \exp \left[-2 \int_{r_2}^{r_3} k(r) dr \right] \quad (1)$$

with the preformation factor P , the normalization factor F

$$F \int_{r_1}^{r_2} \frac{dr}{2k(r)} = 1 \quad (2)$$

and the wave number $k(r)$

$$k(r) = \sqrt{\frac{2\mu}{\hbar^2} |E - V(r)|}. \quad (3)$$

μ is the reduced mass and E is the decay energy of the α -decay which was taken from the mass table of ref. [10]

^a e-mail: WidmaierMohr@compuserve.de

and the recent experimental results of [1,2]. The r_i are the classical turning points. For $0^+ \rightarrow 0^+$ s -wave decay the inner turning point is at $r_1 = 0$. r_2 varies around 7 fm, and r_3 varies strongly depending on the energy. The decay width Γ_α is related to the half-life by the well-known relation $\Gamma_\alpha = \hbar \ln 2 / T_{1/2,\alpha}$. Following eq. (1), the preformation factor may also be obtained as

$$P = \frac{T_{1/2,\alpha}^{\text{calc}}}{T_{1/2,\alpha}^{\text{exp}}}, \quad (4)$$

where Γ_α or $T_{1/2,\alpha}^{\text{calc}}$ are calculated from eq. (1) with $P = 1$. For completeness, I define the here predicted half-life for unknown nuclei as $T_{1/2,\alpha}^{\text{pre}} = T_{1/2,\alpha}^{\text{calc}} / P$. Further details of the model can be found in [11,12].

The potential $V(r)$ in eq. (3) is given by

$$V(r) = V_N(r) + V_C(r) = \lambda V_F(r) + V_C(r), \quad (5)$$

where the nuclear potential V_N is the double-folding potential V_F multiplied by a strength parameter $\lambda \approx 1.1$ – 1.3 [13]. The nuclear densities have been taken from [14] in the same parametrization as in [12] for all nuclei under study. V_C is the Coulomb potential in the usual form of a homogeneously charged sphere with the Coulomb radius R_C chosen the same as the r_{rms} radius of the folding potential V_F . For decays with angular momenta $L \neq 0$ an additional centrifugal potential $V_L = L(L+1)\hbar^2 / (2\mu r^2)$ is used.

The potential strength parameter λ of the folding potential was adjusted to the energy of the α particle in the α emitter $(A+4) = A \otimes \alpha$. The number of nodes of the bound-state wave function was taken from the Wildermuth condition

$$Q = 2N + L = \sum_{i=1}^4 (2n_i + l_i) = \sum_{i=1}^4 q_i, \quad (6)$$

where Q is the number of oscillator quanta, N is the number of nodes and L the relative angular momentum of the α -core wave function, and $q_i = 2n_i + l_i$ are the corresponding quantum numbers of the nucleons in the α cluster. I have taken $q = 4$ for $50 < Z$, $N \leq 82$, $q = 5$ for $82 < Z$, $N \leq 126$ and $q = 6$ for $N > 126$, where Z and N are the proton and neutron number of the daughter nucleus. This leads to $Q = 16$ for the nuclei above ^{100}Sn and $Q = 22$ for the nuclei above ^{208}Pb .

The results for the nuclei $^{108,109,110}\text{Xe}$ and $^{104,105,106}\text{Te}$ above the doubly-magic ^{100}Sn and for $^{216,217,218}\text{Rn}$ and $^{212,213,214}\text{Po}$ above the doubly-magic ^{208}Pb are listed in table 1. The derived preformation factors P are shown in fig. 1 as a function of ΔA_D , where ΔA_D gives the distance from a double shell closure. *E.g.*, the preformation factor for the α -decay $^{106}\text{Te} \rightarrow ^{102}\text{Sn}$ can be found at $\Delta A_D = 2$ because the daughter nucleus ^{102}Sn has two nucleons above the doubly-magic ^{100}Sn . The same value of $\Delta A_D = 2$ is found for the α -decay $^{214}\text{Po} \rightarrow ^{210}\text{Pb}$. Thus, a comparison between the results above $A = 100$ and above $A = 208$ can be done easily.

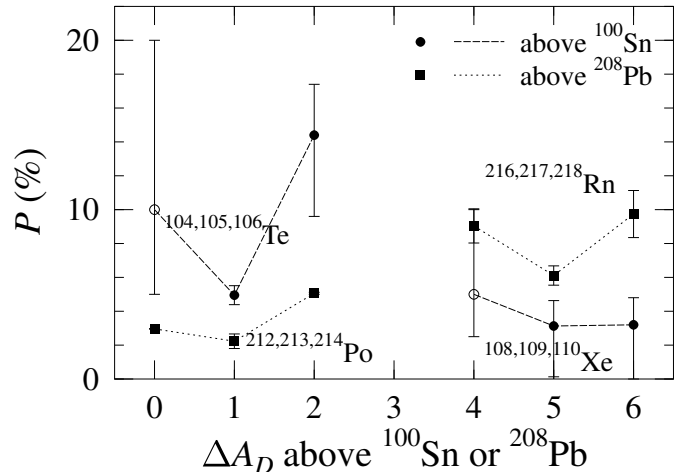


Fig. 1. Comparison of preformation factors P for the α -decays of $^{104,105,106}\text{Te}$ and $^{108,109,110}\text{Xe}$ above doubly-magic ^{100}Sn (circles) and $^{212,213,214}\text{Po}$ and $^{216,217,218}\text{Rn}$ above doubly-magic ^{208}Pb (squares), derived from eq. (4). The open circles for ^{104}Te and ^{108}Xe indicate assumed values: $P = 10\%$ for ^{104}Te and $P = 5\%$ for ^{108}Xe . The lines are to guide the eye only.

The systematic behavior of the potential parameters is one main advantage of the folding potentials. The potential strength parameter λ and the normalized volume integral per interacting nucleon pair

$$J_R = \frac{\lambda}{A_P A_T} \int V_F(r) d^3r \quad (7)$$

show values around $\lambda \approx 1.10$ and $J_R \approx 303 \text{ MeV fm}^3$ for the systems $^{100,101,102}\text{Sn} \otimes \alpha$ and $^{104,105,106}\text{Te} \otimes \alpha$ above $A = 100$; the variations of λ and J_R are less than 1% and allow thus extrapolations with limited uncertainties. The same range of variations of less than 1% is found for the considered systems above $A = 208$, where $\lambda \approx 1.24$ and $J_R \approx 327 \text{ MeV fm}^3$.

The analysis of the $0^+ \rightarrow 0^+$ decays of the even-even systems is straightforward. The ground-state transitions dominate because these transitions have the maximum energy, and the decay is not hindered by an additional centrifugal barrier because $L = 0$. In both decays, $^{217}\text{Rn} \rightarrow ^{213}\text{Po}$ and $^{213}\text{Po} \rightarrow ^{209}\text{Pb}$, the ground-state transitions $9/2^+ \rightarrow 9/2^+$ with $L = 0$ also dominate. However, the analysis of the α -decays $^{109}\text{Xe} \rightarrow ^{105}\text{Te}$ and $^{105}\text{Te} \rightarrow ^{101}\text{Sn}$ requires further study.

Two α groups have been detected in the decay of $^{109}\text{Xe} \rightarrow ^{105}\text{Te}$ which have been interpreted as the $L = 0$ and $L = 2$ decays from the $7/2^+$ ground state of ^{109}Xe to the $5/2^+$ ground state and $7/2^+$ first excited state in ^{105}Te [2]. From eq. (1) one calculates $T_{1/2,\alpha}^{\text{calc}} = 5.71 \times 10^{-4} \text{ s}$ for the $L = 2$ ground-state decay and $T_{1/2,\alpha}^{\text{calc}} = 1.42 \times 10^{-3} \text{ s}$ for the $L = 0$ decay to the first excited state, in both cases using $P = 1$. The theoretical branching is 71% for the ground-state branch and 29% for the branch to the first excited state. This is in excellent agreement with the experimental values of $(70 \pm 6)\%$ for the ground-state branch and $(30 \pm 6)\%$ for the branch to the first excited

Table 1. α -decay half-lives for nuclei above ^{100}Sn and ^{208}Pb .

Decay	$J_i \rightarrow J_f$	E (MeV)	λ	J_R (MeV fm ³)	$T_{1/2}^{\text{exp}}$ or $T_{1/2}^{\text{pre}}$ (s)	$T_{1/2}^{\text{calc}}$ (s)	P (%)
$^{218}\text{Rn} \rightarrow ^{214}\text{Po}$	$0^+ \rightarrow 0^+$	7.263	1.2431	328.2	$(3.5 \pm 0.5) \times 10^{-2}$	3.41×10^{-3}	9.74 ± 1.39
$^{217}\text{Rn} \rightarrow ^{213}\text{Po}$	$9/2^+ \rightarrow 9/2^+$	7.887	1.2390	327.2	$(5.4 \pm 0.5) \times 10^{-4}$	3.30×10^{-5}	6.11 ± 0.57
$^{216}\text{Rn} \rightarrow ^{212}\text{Po}$	$0^+ \rightarrow 0^+$	8.200	1.2386	327.2	$(4.5 \pm 0.5) \times 10^{-5}$	4.07×10^{-6}	9.04 ± 1.01
$^{214}\text{Po} \rightarrow ^{210}\text{Pb}$	$0^+ \rightarrow 0^+$	7.834	1.2384	327.3	$(1.64 \pm 0.02) \times 10^{-4}$	8.32×10^{-6}	5.06 ± 0.06
$^{213}\text{Po} \rightarrow ^{209}\text{Pb}$	$9/2^+ \rightarrow 9/2^+$	8.536	1.2333	326.1	$(4.2 \pm 0.8) \times 10^{-6}$	9.38×10^{-8}	2.23 ± 0.43
$^{212}\text{Po} \rightarrow ^{208}\text{Pb}$	$0^+ \rightarrow 0^+$	8.954	1.2316	325.7	$(2.99 \pm 0.02) \times 10^{-7}$	8.70×10^{-9}	2.96 ± 0.02
$^{110}\text{Xe} \rightarrow ^{106}\text{Te}$	$0^+ \rightarrow 0^+$	3.885	1.0981	302.4	$\approx 4 \times 10^{-1^a}$	1.29×10^{-2}	≈ 3.2
$^{109}\text{Xe} \rightarrow ^{105}\text{Te}$	$7/2^+ \rightarrow 7/2^+$	4.067	1.1006	303.2	$(1.3 \pm 0.2) \times 10^{-2}$	$1.42 \times 10^{-3^b}$	$\approx 3^b$
$^{108}\text{Xe} \rightarrow ^{104}\text{Te}$	$0^+ \rightarrow 0^+$	4.65 ^c	1.099	303.4	$\approx 60 \mu\text{s}^{c,d}$	$\approx 3 \times 10^{-6^d}$	$\approx 5^e$
$^{106}\text{Te} \rightarrow ^{102}\text{Sn}$	$0^+ \rightarrow 0^+$	4.290	1.1026	304.5	$(6.0_{-1.0}^{+3.0}) \times 10^{-5}$	8.66×10^{-6}	$14.4_{-4.8}^{+3.0}$
$^{105}\text{Te} \rightarrow ^{101}\text{Sn}$	$5/2^+ \rightarrow 5/2^+$	4.889	1.1006	304.1	$(6.2 \pm 0.7) \times 10^{-7}$	3.07×10^{-8}	4.95 ± 0.56
$^{104}\text{Te} \rightarrow ^{100}\text{Sn}$	$0^+ \rightarrow 0^+$	5.42 ^c	1.100	304.0	$\approx 5 \text{ ns}^c$	$\approx 5 \times 10^{-10}$	$\approx 10^e$

^a α -decay branch only.^b Branching to $7/2^+$: see sect. 2.^c Predicted values; see sect. 3.^d Huge uncertainty from unknown energy E ; see sect. 3.^e Assumed values; see fig. 1.

state [2]. In fig. 1 I show the preformation factor P in ^{109}Xe for the $L = 0$ decay only because all the other decays in fig. 1 have the same $L = 0$.

For the α -decay $^{105}\text{Te} \rightarrow ^{101}\text{Sn}$ only one α group has been detected in [2], and an upper limit of 5% is given for other decay branches. The α -decay strength increases with increasing energy and decreasing angular momentum. If only one decay branch is observed, one may conclude that this branch corresponds to a $L = 0$ ground-state transition. Consequently, $J^\pi(^{101}\text{Sn}) = J^\pi(^{105}\text{Te}) = 5/2^+$ [2]. This is in agreement with a recent theoretical prediction [15]. The derived values for the potential strength parameter λ and the volume integral J_R fit into the systematics and thus strengthen the above tentative spin assignment.

The results in fig. 1 and table 1 confirm the super-allowed nature of α -decay near the doubly-magic ^{100}Sn . For $^{216,217,218}\text{Rn}$ one finds preformation values P between about 5% and 10%. Surprisingly, P slightly decreases for $^{212,213,214}\text{Po}$ to values between about 2% and 5% when approaching the doubly-magic daughter nucleus ^{208}Pb . For $^{109,110}\text{Xe}$ relatively small values of $P \approx 3\%$ are found. When approaching the doubly-magic daughter ^{100}Sn , the preformation values P show the expected behavior and increase to about 5% to 15% for $^{105,106}\text{Te}$. A comparison between the preformation factors P for the Po isotopes and the Te isotopes shows that

$$P(\text{Te}) \approx 3 \times P(\text{Po}) \quad (8)$$

in agreement with the conclusions of [1, 2].

3 Predicted half-lives of ^{104}Te and ^{108}Xe

The systematic behavior of the potential parameters λ and J_R in combination with the shown preformation factors P (see fig. 1) enables the extrapolation to the decays $^{108}\text{Xe} \rightarrow ^{104}\text{Te} \rightarrow ^{100}\text{Sn}$ with limited uncertainties.

For the prediction of the α -decay energies I use a local potential which is adjusted to the neighboring nuclei.

The potentials for $^{105}\text{Te} = ^{101}\text{Sn} \otimes \alpha$ and $^{106}\text{Te} = ^{102}\text{Sn} \otimes \alpha$ are practically identical. From the average $J_R = 304.29 \text{ MeV fm}^3$ one obtains the α -decay energy of ^{104}Te $E = 5.354 \text{ MeV}$, whereas a linear extrapolation yields a slightly weaker potential $J_R = 303.76 \text{ MeV fm}^3$ and slightly higher energy $E = 5.481 \text{ MeV}$. Combining these results, a reasonable prediction of the α -decay energy of ^{104}Te is $E = 5.42 \pm 0.07 \text{ MeV}$.

From the lower decay energy $E = 5.354 \text{ MeV}$ one obtains $T_{1/2,\alpha}^{\text{calc}} = 7.87 \times 10^{-10} \text{ s}$ from eq. (1) with $P = 1$; the higher decay energy yields $T_{1/2,\alpha}^{\text{calc}} = 3.13 \times 10^{-10} \text{ s}$. The uncertainty of the α -decay energy of about 70 keV translates to an uncertainty in the calculated half-life of about a factor of 1.5. For a prediction of the α -decay half-life one has to find a reasonable assumption for the preformation factor P . Following the pattern of P in fig. 1, I use $P = 10\%$ with an estimated uncertainty of a factor of two. Combining the above findings, the predicted half-life of ^{104}Te is $T_{1/2,\alpha}^{\text{pre}} = 5 \text{ ns}$ with an uncertainty of about a factor three. The uncertainty of the predicted half-life is composed of similar contributions for the unknown α -decay energy and the assumed preformation factor P .

The potentials for $^{109}\text{Xe} = ^{105}\text{Te} \otimes \alpha$ and $^{110}\text{Xe} = ^{106}\text{Te} \otimes \alpha$ change by about 1 MeV fm^3 ; this is still very similar, but not as close as in the above $^{105}\text{Te} = ^{101}\text{Sn} \otimes \alpha$ and $^{106}\text{Te} = ^{102}\text{Sn} \otimes \alpha$ cases. Repeating the above procedure, one finds the α -decay energy $E = 4.792 \text{ MeV}$ from the average $J_R = 302.82 \text{ MeV fm}^3$ and $E = 4.506 \text{ MeV}$ from the extrapolated $J_R = 303.96 \text{ MeV fm}^3$. The calculated half-lives using $P = 1$ are $T_{1/2,\alpha}^{\text{calc}} = 7.40 \times 10^{-7} \text{ s}$ for the higher energy $E = 4.792 \text{ MeV}$ and $T_{1/2,\alpha}^{\text{calc}} = 1.18 \times 10^{-5} \text{ s}$ for the lower energy $E = 4.506 \text{ MeV}$. Combining these

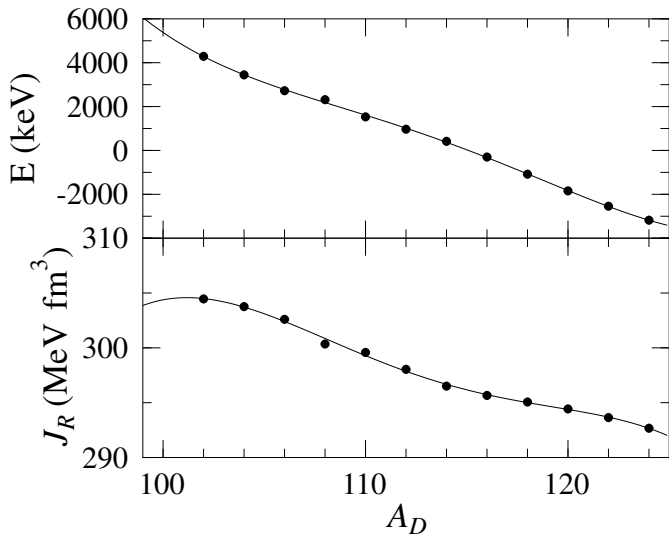


Fig. 2. Volume integral J_R and energy E in dependence on the mass number A_D from ^{102}Sn to ^{124}Sn (See text).

results, the α -decay energy is $E = 4.65 \pm 0.15$ MeV. Together with a preformation factor of about $P = 5\%$ the α -decay half-life is predicted to be of the order of $100 \mu\text{s}$. However, the uncertainty of the decay energy of 150 keV leads to an uncertainty in the half-life of a factor of 4; thus it is impossible to predict the α -decay half-life of ^{108}Xe better than this uncertainty.

It is interesting to compare the predictions for the α -decay properties of ^{104}Te with the results of [3]. In [3] the α -decay energy is linearly extrapolated from the neighboring even-even Te isotopes $^{106,108,110}\text{Te}$ leading to $E = 5.053$ MeV. I have repeated this procedure for the Te isotopes ^{106}Te to ^{126}Te . The α -decay energies and derived volume integrals J_R are shown in fig. 2. For an extrapolation to the α -decay of ^{104}Te I have fitted the data in fig. 2 using a polynomial

$$E(A_D) = \sum_{i=0}^n a_i (A_D - 100)^i \quad (9)$$

and a corresponding formula for the volume integral J_R . It has turned out that the reduced χ^2 of the fit improves when one increases the number n up to $n = 4$; no further significant improvement is found for larger values of n . These fourth-order polynomials for E and J_R are shown as lines in fig. 2. The resulting numbers for $A_D = 100$, *i.e.* the $^{104}\text{Te} \rightarrow ^{100}\text{Sn}$ α -decay, are $E = 5.379$ MeV and $J_R = 304.4$ MeV fm^3 which is within the error bars of the values derived above from the neighboring potentials.

Because of the higher α -decay energy derived in this work, the α -decay half-life of ^{104}Te is about a factor of 10 shorter compared to the predictions of [3]. Experimental data are required to distinguish between the predictions of this work and ref. [3].

The results for ^{108}Xe roughly agree with the predictions in [3]: Xu *et al.* predict the α -decay energy $E = 4.44$ MeV compared to $E = 4.65 \pm 0.15$ MeV in this work,

Table 2. Comparison of α -decay energies from a local extrapolation using folding potentials (this work) to predictions of global mass formula [16–20]. All energies are given in MeV.

	Exp. or this work	FRDM [17]	HFB-1 [18, 16]	HFB-2 [19]	DZ [20]
^{104}Te	5.42 ± 0.07^a	6.12	4.85	4.68	5.24
^{105}Te	4.89	6.31	4.91	4.28	4.91
^{106}Te	4.29	6.01	4.72	4.16	4.60
^{108}Xe	4.65 ± 0.15^a	5.53	4.69	4.38	4.93
^{109}Xe	4.22^b	4.81	4.23	4.03	4.62
^{110}Xe	3.89	4.61	3.60	3.71	4.33

^a Predicted from folding potential.

^b From ground state in ^{109}Xe to ground state in ^{105}Te .

and the predicted half-life in [3] is between 150 and $290 \mu\text{s}$ which should be compared to the predicted half-life of $T_{1/2,\alpha}^{\text{pre}} = 236 \mu\text{s}$ derived from the lower limit $E = 4.5$ MeV of the energy with $P = 5\%$.

4 Comparison to mass formulae

The α -decay energies of the folding calculation may be compared to predictions from global mass formulae. Here I restrict myself to the three selected mass formulae of the so-called Reference Input Parameter Library RIPL-2 of the IAEA [16] which are the Finite Range Droplet Model (FRDM) [17], the Hartree-Fock-Bogoliubov (HFB) method [18] in the versions of [16] and its latest update [19], and the simple 10-parameter formula of Duflo and Zuker (DZ) [20]. The results are listed in table 2.

The FRDM predictions seem to overestimate the experimental α -decay energies slightly, especially when approaching the doubly-magic core ^{100}Sn . The predictions of HFB-1 and HFB-2 are close to the experimental values, and also the simple 10-parameter parametrization DZ is in reasonable agreement with the data. The predictions from the folding potential calculation for ^{104}Te and ^{108}Xe are close to the average values of the above global mass models [16–20].

5 Accuracy of semi-classical half-lives

The results which are presented in table 1 and fig. 1 have been obtained using the semi-classical approximation of eq. (1) for the decay width Γ_α . From a fully quantum-mechanical analysis the decay width Γ_α is related to the energy dependence of a resonant scattering phase shift $\delta_L(E)$ by

$$\delta_L(E) = \arctan \frac{\Gamma_\alpha}{2(E_R - E)}. \quad (10)$$

In practice, it is difficult to determine widths of the order of $1 \mu\text{eV}$ at energies of the order of several MeV because of numerical problems. For the system $^{104}\text{Te} = ^{100}\text{Sn} \otimes \alpha$ such an analysis is possible at the limits of numerical stability.

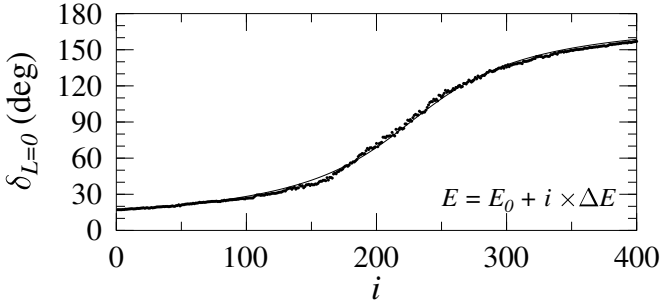


Fig. 3. Phase shift δ_L for the $L = 0$ partial wave for the system $^{104}\text{Te} = ^{100}\text{Sn} \otimes \alpha$. The derived width from eq. (10) is $\Gamma = 1.36 \times 10^{-12}$ MeV. Note the extremely small stepsize of the calculation of $\Delta E = 1.0 \times 10^{-14}$ MeV! See text for details.

In fig. 3 the resonant behavior of the s -wave phase shift $\delta_{L=0}(E)$ is shown around the resonance energy $E_R = 5.481$ MeV which is obtained in the potential with $J_R = 303.76$ MeV (see sect. 3). The dots are obtained from solving the Schrödinger equation at $E = E_0 + i \times \Delta E$ with $E_0 = 5.481305851985$ MeV and $\Delta E = 10^{-14}$ MeV. The full line is a fit of data using eq. (10) where the resonance energy E_R and the width Γ_α have been adjusted. This yields $\Gamma_\alpha = 1.36 \mu\text{eV}$ and a corresponding half-life of $T_{1/2,\alpha}^{\text{calc}} = 0.336$ ns. The semi-classical approximation in eq. (1) gives $T_{1/2,\alpha}^{\text{calc}} = 0.313$ ns which is about 8% lower than the value from the fully quantum-mechanical calculation.

The validity of the semi-classical approximation for Γ_α in eq. (1) is confirmed for the α -decay of ^{104}Te by the above analysis of the scattering phase shift $\delta_L(E)$ with an uncertainty of less than 10%. For two other nuclei (^8Be and ^{212}Po) the semi-classical approximation deviates by about 30% from the fully quantum-mechanical value. In all cases the semi-classical half-life is slightly shorter than the fully quantum-mechanical result.

In a detailed study on proton-decay half-lives of proton-rich nuclei [21] it has been shown that the semi-classical approximation agrees within about $\pm 10\%$ with the result of a direct calculation of the transition amplitude using the distorted-wave Born approximation (DWBA) formalism. Surprisingly, the agreement between the quantum-mechanical DWBA calculation and the semi-classical result becomes worse in [21] when an improved normalization factor from eq. (25) of [21] is used compared to the simple normalization factor in eq. (24) of [21] or eq. (2) in this work: For the case of ^{104}Te , the α -decay half-life in the semi-classical calculation changes from 0.313 ns using eq. (2) to 0.231 ns using eq. (25) of [21]; thus, the findings in [21] are confirmed.

6 Properties of $^{104}\text{Te} = ^{100}\text{Sn} \otimes \alpha$

From the given potential of the system $^{104}\text{Te} = ^{100}\text{Sn} \otimes \alpha$ it is not only possible to determine the α -decay half-life of the ground state. Following the formalism in [22], energies and electromagnetic decay properties of excited states in ^{104}Te can be predicted.

Table 3. Excitation energies $E_x = E - E(0^+)$ of excited states in $^{104}\text{Te} = ^{100}\text{Sn} \otimes \alpha$ with $Q = 16, 17$, and 18.

J^π	Q	N	L	λ	E (keV)	E_x (keV)
0^+	16	8	0	1.1005	5354.2	0.0
2^+	16	7	2	1.0915	6003.5	649.3
4^+	16	6	4	1.0825	6739.6	1385.4
6^+	16	5	6	1.0735	7565.2	2211.0
8^+	16	4	8	1.0645	8477.2	3123.0
10^+	16	3	10	1.0555	9469.2	4115.0
12^+	16	2	12	1.0465	10543.2	5189.0
14^+	16	1	14	1.0375	11731.2	6377.0
16^+	16	0	16	1.0285	13097.1	7742.9
1^-	17	8	1	1.0960	10951.4	5597.2
0^+	18	9	0	1.1005	≈ 15 MeV ^a	≈ 10 MeV ^a

^a Very broad.

The ground-state wave function of ^{104}Te is characterized by $Q = 2N + L = 16$, see eq. (6). Further members of this $Q = 16$ band are expected with $J^\pi = 2^+, 4^+, \dots, 16^+$. It has been observed that the potential strength parameter λ has to be varied slightly to obtain an excellent prediction of the excitation energies:

$$\lambda(L) = \lambda(L = 0) - c \times L \quad (11)$$

with the constant $c \approx (3-5) \times 10^{-3}$ for neighboring $N = 50 \otimes \alpha$ nuclei $^{94}\text{Mo} = ^{90}\text{Zr} \otimes \alpha$ [7, 8], $^{93}\text{Nb} = ^{89}\text{Y} \otimes \alpha$ [23], neighboring $Z = 50$ nuclei $^{116}\text{Te} = ^{112}\text{Sn} \otimes \alpha$, and the systems $^{20}\text{Ne} = ^{16}\text{O} \otimes \alpha$ [24], $^{44}\text{Ti} = ^{40}\text{Ca} \otimes \alpha$ [13], and $^{212}\text{Po} = ^{208}\text{Pb} \otimes \alpha$ [25].

For the following analysis I adopt $\lambda = 1.1005$ which corresponds to $J_R = 304.29$ MeV fm³ from the average of the two neighboring systems $^{105,106}\text{Te} = ^{101,102}\text{Sn} \otimes \alpha$ and $c = (4.5 \pm 0.3) \times 10^{-3}$ from the neighboring nuclei ^{93}Nb , ^{94}Mo , and ^{116}Te above $N = 50$ or $Z = 50$ cores. Because the predicted excitation energies $E_x = E - E(0^+)$ (see table 3) are relative to the ground-state energy, the excitation energies do not change significantly when one varies $\lambda(L = 0)$ or J_R within the given uncertainties.

The first excited 2^+ state in ^{104}Te is found at $E_x = 649$ keV. From the uncertainty of the constant c in eq. (11) one can derive a very small uncertainty for the potential strength $\lambda(L = 2)$ and a resulting uncertainty of about 40 keV for the excitation energy E_x for the first 2^+ state. Somewhat larger uncertainties are found for $\lambda(L > 2)$; consequently, the uncertainty of the predicted excitation energies increases up to about 400 keV for the 16^+ state at $E_x = 8.55$ MeV.

In addition, the 1^- and 0^+ band heads of the bands with $Q = 17$ and $Q = 18$ are predicted at energies around $E_x = 5.60$ MeV and about 10 MeV. The 0^+ state is very broad. It is difficult to estimate the uncertainty of the predicted energies of the 1^- and 0^+ states with $Q = 17$ and $Q = 18$ because usually the potential strength has to be slightly readjusted to obtain a good description of such bands. A rough estimate for the uncertainty is about 1 MeV which corresponds to an uncertainty of about 2% for the potential strength parameter λ .

Following the formalism of ref. [22], reduced transition strengths of 10.1 W.u., 14.0 W.u., and 14.1 W.u. are calculated for the $2^+ \rightarrow 0^+$, $4^+ \rightarrow 2^+$, and $6^+ \rightarrow 4^+$ transitions in ^{104}Te . The corresponding radiation widths Γ_γ are slightly larger than the direct α -decay widths from the excited states in ^{104}Te to the ground state in ^{100}Sn . The γ -decay branching ratio

$$b_\gamma = \frac{\Gamma_\gamma}{\Gamma_\gamma + \Gamma_\alpha^{\text{pre}}} \quad (12)$$

is between 86% and 93% for the 2^+ state, between 62% and 76% for the 4^+ state, and between 48% and 62% for the 6^+ state. This is an extremely important result for future experiments! If the γ -decay branch b_γ of the first 2^+ state were small (*e.g.*, of the order of a few per cent), it would be extremely difficult to produce ^{104}Te in its ground state because ^{104}Te produced in excited states could directly decay to the ^{100}Sn ground state by α emission.

It is interesting to note that the predicted branchings b_γ are not very sensitive to the predicted excitation energy. *E.g.*, if the excitation energy of the first excited 2^+ state in ^{104}Te is $E_x = 1$ MeV, the radiation width Γ_γ increases with E_x^5 by a factor of about 9 and the width Γ_α increases by a factor of about 8 because of the reduced Coulomb barrier. Thus, b_γ values close to unity are very likely. Consequently, a direct production reaction like *e.g.* $^{50}\text{Cr}(^{58}\text{Ni}, 4n)^{104}\text{Te}$ similar to the experiment in [1] should be feasible. However, only the indirect production via the α -decay of ^{108}Xe in a reaction like, *e.g.*, $^{54}\text{Fe}(^{58}\text{Ni}, 4n)^{108}\text{Xe}$ similar to [2] ensures the production of ^{104}Te in its ground state.

7 Conclusions

The systematic properties of folding potentials provide a powerful tool for the analysis of the system $^{104}\text{Te} = ^{100}\text{Sn} \otimes \alpha$ above the doubly-magic ^{100}Sn core. In particular, α -decay energies and half-lives can be predicted with relatively small uncertainties. The predicted α -decay energy for ^{104}Te is $E = 5.42 \pm 0.07$ MeV, and the corresponding half-life is $T_{1/2, \alpha}^{\text{pre}} = 5$ ns with an uncertainty of a factor of three.

Excitation energies and decay properties of the members of the $Q = 16$ rotational band in ^{104}Te are calculated, and the predicted values have small uncertainties. For the first excited 2^+ state in ^{104}Te one obtains $E_x = 650 \pm 40$ keV. The γ -decay strength to the ground state in ^{104}Te is about 10 Weisskopf units. The corresponding radiation width Γ_γ is about a factor of 10 larger than the α -decay width Γ_α to the ground state in ^{100}Sn .

The finding that Γ_γ is larger than Γ_α for excited states in ^{104}Te is important for the experimental production of ^{104}Te in its ground state and the measurement of the α -decay half-life of ^{104}Te . The condition $\Gamma_\gamma > \Gamma_\alpha$ allows to use reactions which produce ^{104}Te in excited states because these states preferentially decay to the ^{104}Te ground state. However, only the indirect production of ^{104}Te via the α -decay of ^{108}Xe safely guarantees that ^{104}Te is produced in its ground state.

I thank Z. Ren, Gy. Gyürky, and Zs. Fülöp for encouraging discussions and the referees for their constructive reports.

References

1. D. Seweryniak, K. Starosta, C.N. Davids, S. Gros, A.A. Hecht, N. Hoteling, T.L. Khoo, K. Lagergren, G. Lotay, D. Peterson, A. Robinson, C. Vaman, W.B. Walters, P.J. Woods, S. Zhu, Phys. Rev. C **73**, 061301(R) (2006).
2. S.N. Liddick, R. Grzywacz, C. Mazzocchi, R.D. Page, K.P. Rykaczewski, J.C. Batchelder, C.R. Bingham, I.G. Darby, G. Drafta, C. Goodin, C.J. Gross, J.H. Hamilton, A.A. Hecht, J.K. Hwang, S. Ilyushkin, D.T. Joss, A. Korgul, W. Królas, K. Lagergren, K. Li, M.N. Tantawy, J. Thomson, J.A. Winger, Phys. Rev. Lett. **97**, 082501 (2006).
3. C. Xu, Z. Ren, Phys. Rev. C **74**, 037302 (2006).
4. Zs. Fülöp, Gy. Gyürky, Z. Máté, E. Somorjai, L. Zolnai, D. Galaviz, M. Babilon, P. Mohr, A. Zilges, T. Rauscher, H. Oberhammer, G. Staudt, Phys. Rev. C **64**, 065805 (2001).
5. G.G. Kiss, Zs. Fülöp, Gy. Gyürky, Z. Máté, E. Somorjai, D. Galaviz, A. Kretschmer, K. Sonnabend, A. Zilges, Eur. Phys. J. A **27**, 197 (2006).
6. D. Galaviz, Zs. Fülöp, Gy. Gyürky, Z. Máté, P. Mohr, T. Rauscher, E. Somorjai, A. Zilges, Phys. Rev. C **71**, 065802 (2005).
7. S. Ohkubo, Phys. Rev. Lett. **74**, 2176 (1995).
8. F. Michel, S. Ohkubo, G. Reidemeister, Prog. Theor. Phys. Suppl. **132**, 7 (1998).
9. S.A. Gurvitz, G. Kälbermann, Phys. Rev. Lett. **59**, 262 (1987).
10. A.H. Wapstra, G. Audi, C. Thibault, Nucl. Phys. A **729**, 129 (2003).
11. P. Mohr, Phys. Rev. C **61**, 045802 (2000).
12. P. Mohr, Phys. Rev. C **73**, 031301(R) (2006).
13. U. Atzrott, P. Mohr, H. Abele, C. Hillenmayer, G. Staudt, Phys. Rev. C **53**, 1336 (1996).
14. H. de Vries, C.W. de Jager, C. de Vries, At. Data Nucl. Data Tables **36**, 495 (1987).
15. O. Kavatsyuk *et al.*, GSI Report 2006-1 (to be published).
16. T. Belgia *et al.*, *Handbook for calculations of nuclear reaction data*, RIPL-2, IAEA-TECDOC-1506 (IAEA, Vienna, 2006) available online at <http://www-nds.iaea.org/RIPL-2/>.
17. P. Möller, J.R. Nix, W.D. Myers, W.J. Swiatecki, At. Data Nucl. Data Tables **59**, 185 (1995); <http://t2.lanl.gov/data/astro/molnix96/molnix.html>.
18. M. Samyn, S. Goriely, P.-H. Heenen, J.M. Pearson, F. Tondeur, Nucl. Phys. A **700**, 142 (2001).
19. S. Goriely, M. Samyn, J.M. Pearson, M. Onsi, Nucl. Phys. A **750**, 425 (2005); <http://www-astro.ulb.ac.be/Nucdata/Masses/>.
20. J. Duflo, A.P. Zuker, Phys. Rev. C **52**, 23 (1995).
21. S. Åberg, P.B. Semmes, W. Nazarewicz, Phys. Rev. C **56**, 1762 (1997); **58**, 3011 (1998).
22. B. Buck, A.C. Merchant, S.M. Perez, Phys. Rev. C **51**, 559 (1995).
23. G.G. Kiss *et al.*, in preparation.
24. H. Abele, G. Staudt, Phys. Rev. C **47**, 742 (1993).
25. F. Hoyler, P. Mohr, G. Staudt, Phys. Rev. C **50**, 2631 (1994).